REPORT DOCUMENTATION PAGE

Form Approved
OMB No. 0704-0188

1. REPORT DATE *(DD-MM-YYYY)* 14-12-2007	2. REPORT TYPE Journal Article	3. DATES COVERED *(From - To)* Dec 07 – Jan 08

4. TITLE AND SUBTITLE

Molecular Beam Epitaxy on Gas Cluster Ion Beam Prepared GaSb Substrates: Towards Improved Surfaces and Interfaces

5a. CONTRACT NUMBER
IN-HOUSE

5b. GRANT NUMBER

5c. PROGRAM ELEMENT NUMBER
61102F

6. AUTHOR(S)

*Kannan Krishnaswami, **Shivashankar R. Vangala, Helen M. Dauplaise, ***Lisa P. Allen,***Gordon Dallas, ***Daniel Bakken, David F. Bliss, and **William D. Goodhue

5d. PROJECT NUMBER
2305

5e. TASK NUMBER
HC

5f. WORK UNIT NUMBER
01

7. PERFORMING ORGANIZATION NAME(S) AND ADDRESS(ES)
Optoelectronic Technology Branch, 80 Scott Drive, Hanscom AFB, MA 01731-2909
*Pacific Northwest National Laboratory, 902 Battelle Boulevard, Richland, WA 99352
**Dept. of Physics, Photonics Center, University of Massachusetts, Lowell, MA 01854,
***Galaxy Compound Semiconductors, 9922 E. Montgomery Avenue, Spokane, WA

8. PERFORMING ORGANIZATION REPORT

9. SPONSORING / MONITORING AGENCY NAME(S) AND ADDRESS(ES)
Electromagnetics Technology Division   Source Code: 437890
Sensors Directorate
Air Force Research Laboratory
80 Scott Drive
Hanscom AFB MA 01731-2909

10. SPONSOR/MONITOR'S ACRONYM(S)
AFRL/RYHC

11. SPONSOR/MONITOR'S REPORT NUMBER(S)
AFRL-RY-HS-TP-2008-0009

12. DISTRIBUTION / AVAILABILITY STATEMENT
DISTRIBUTION A: APPROVED FOR PUBLIC RELEASE; DISTRIBUTION UNLIMITED.

14. ABSTRACT
We report results of a surface modification process for (100) GaSb using gas cluster ion beams(GCIB) that removes chemical mechanical polish (CMP) induced surface damage and replaces the native oxide with an engineered surface oxide, the composition of which depends on the reactive gas employed. X-ray photoelectron spectroscopy of O_2-, CF_4/O_2-, and HBr-GCIB surface oxides is presented indicating the presence of mixed Ga- and Sb-oxides, with mostly Ga-oxides at the interface, desorbing at temperatures ranging 530°C to 560°C. Cross-sectional transmission electron microscopy of molecular beam epitaxy grown GaSb/AlGaSb layers showed that the HBr-GCIB surface produced a smooth dislocation-free substrate-to-epi transition with no discernable interface. Topography of epi surfaces, using atomic force microscopy, showed that GCIB surfaces resulted in characteristic step-terrace formations comprising monatomic steps and wide terraces. The HBr-GCIB process can be easily adapted to a large scale manufacturing process to produce epi-ready GaSb substrates.

15. SUBJECT TERMS
 Surface processes, Molecular beam epitaxy, gas cluster ion beam, antimonides, surface oxides, GaSb

16. SECURITY CLASSIFICATION OF:			17.LIMITATION OF ABSTRACT	18.NUMBER OF PAGES	19a. NAME OF RESPONSIBLE PERSON David Bliss
a. REPORT Unclassified	**b. ABSTRACT** Unclassified	**c. THIS PAGE** Unclassified	SAR	9	**19b. TELEPHONE NUMBER** *(include area code)* N/A

Standard Form 298 (Rev. 8-98)
Prescribed by ANSI Std. Z39.18

Molecular beam epitaxy on gas cluster ion beam-prepared GaSb substrates: Towards improved surfaces and interfaces

Kannan Krishnaswami[a,*], Shivashankar R. Vangala[b], Helen M. Dauplaise[c], Lisa P. Allen[d], Gordon Dallas[d], Daniel Bakken[d], David F. Bliss[c], William D. Goodhue[b]

[a]*Pacific Northwest National Laboratory, 902 Battelle Boulevard, Richland, WA 99352, USA*
[b]*Department of Physics, Photonics Center, University of Massachusetts, Lowell, MA 01854, USA*
[c]*Air Force Research Laboratory/SNHC, Hanscom Air Force Base, MA 01731, USA*
[d]*Galaxy Compound Semiconductors, Inc., 9922 E. Montgomery Avenue, Spokane, WA, USA*

Available online 14 December 2007

Abstract

We report results of a surface modification process for (1 0 0) GaSb using a gas cluster ion beam (GCIB) technique that removes chemical mechanical polish (CMP)-induced surface damage and replaces the native oxide with an engineered surface oxide, the composition of which depends on the reactive gas employed. X-ray photoelectron spectroscopy of O_2-, CF_4/O_2-, and HBr-GCIB surface oxides is presented indicating the presence of mixed Ga- and Sb-oxides, with mostly Ga-oxides at the interface, that desorb at temperatures ranging 530–560 °C. Cross-sectional transmission electron microscopy of molecular-beam epitaxy grown GaSb/AlGaSb layers showed that the HBr-GCIB surface produced a smooth dislocation-free substrate-to-epi transition with no discernable interface. Topography of epi surfaces, using atomic force microscopy, showed that GCIB surfaces resulted in characteristic step-terrace formations comprising monatomic steps and wide terraces. The HBr-GCIB process can be easily adapted to a large-scale manufacturing process to produce epi-ready GaSb substrates.
© 2008 Elsevier B.V. All rights reserved.

1. Introduction

Due to high electron mobilities and a wide range of bandgaps (0.2–2.2 eV) [1], there is significant interest in developing mid-infrared optoelectronic and low-power electronic devices based on the 6.1 Å material system. One of the key problems inhibiting the wider use of this material system is the lack of substrates with appropriate surfaces for epitaxial growth. GaSb is the available substrate of choice for near lattice-matched epitaxial growth though standard chemical mechanical polishing (CMP) results in surface scratches and sub-surface damage accompanied by a tenacious oxide that does not easily desorb.

In the past, surface preparation methods to replace CMP produced surface oxides with thinner, more stable, and thermally desorbable surface oxides have included wet chemistry [2–5], sulfide-based surface passivation [6,7], ultraviolet radiation [8], and dry ion etch techniques [9]. Although these methods have shown varying degrees of success, none can be considered as a final polish. Thus, there exists a need for developing a surface preparation technique for producing "epi-ready" GaSb substrates.

Recently, gas cluster ion beam (GCIB) processing of the GaSb (1 0 0) substrates demonstrated a reduction of surface roughness in combination with producing oxide layers, the stoichiometry of which depends on the reactive gas species [10]. Epitaxial growth on GCIB processed substrates showed improved substrate/epi interfaces, when compared to CMP surfaces, with the presence of a dislocation layers that was attributed to incomplete oxide desorbtion [11]. An

---

*Corresponding author. Tel.: +1 509 375 4597; fax: +1 509 375 2688.
E-mail address: kannan.krishnaswami@pnl.gov (K. Krishnaswami).

alternate surface preparation method using Br-ion beam-assisted etching (Br-IBAE) was also implemented [12]. Though the Br-IBAE process increased surface roughness of the GaSb substrates, epitaxial growth showed smooth, dislocation-free substrate-to-epi transitions with no discernable interface, attributed to complete oxide desorption. This suggested that GaSb's tendency to self-planarize could be exploited to relax surface flatness requirements (<2 Å) and instead place emphasis on well behaved and easily desorbable oxide layers. Thus, we combined the GCIB and Br-IBAE methods to develop the HBr-GCIB process to prepare GaSb surfaces for epitaxial growth with the desorbable oxides.

In this paper, we report results of oxide composition and desorption on the GaSb substrates prepared by CMP, Br-IBAE, and GCIB processes incorporating O_2, CF_4/O_2, HBr gases. Further, we provide experimental results of epitaxial growth on Br-IBAE and HBr-GCIB processed GaSb surfaces showing smooth dislocation-free substrate/epi interfaces. Finally, we analyze episurface morphology that emphasizes the need for smooth GaSb substrates for the epitaxial growth.

2. Surface treatment of GaSb

CMP-processed GaSb substrates cut to within $\pm 0.5°$ of the (1 0 0) crystal orientation were commercially procured for this study. An incoming surface inspection revealed an average roughness ranging from 3 to 10 Å with shallow surface scratches and associated sub-surface damage. The substrates were then GCIB and Br-IBAE processed, details of which can be found in Refs. [11,12], respectively. The process parameters employed were as follows:

- O_2-GCIB process—10 keV etch step followed by a 3 keV smoothing step with a total charge fluence of 4×10^{15} ions/cm^2;
- CF_4/O_2-GCIB process—comprising 5% CF_4 and 95% O_2 gas, 10 keV etch step followed by a 3 keV smoothing step with a total charge fluence of 4×10^{15} ions/cm^2;
- HBr-GCIB process—comprising 1% HBr and 99% Ar gas, 10 keV etch step followed by a 5 keV smoothing step with a total charge fluence of 1×10^{15} ions/cm^2; and
- Br-IBAE process—Beam voltage of 600 V, beam current of 3 mA, beam current at sample (Faraday cup) was 10 μA, argon flow rate of 3 sccm, and Br back pressure of 1 μTorr.

All the processed GaSb substrates were characterized using atomic force microscopy (AFM), X-ray photoelectron spectroscopy (XPS) with depth profiling, and spectroscopic ellipsometry (SE) to measure surface roughness, oxide composition, and oxide thickness, respectively.

3. Surface roughness results

Average surface roughness (R_a), root-mean-square roughness (R_{rms}), and peak-to-valley range (ΔZ) of CMP,

GCIB, and Br-IBAE processed GaSb surfaces were measured using a Digital Nanoscope AFM. Table 1 provides typical measurements for pre- and post-processed surfaces, with a scan resolution of 10×10 μm^2, sample areas relevant to device metrology. AFM measurements show that both the O_2- and HBr-GCIB processes tend to minimally increase the surface roughness, as compared with the pre-processed (CMP) surfaces, while the CF_4/O_2-GCIB process showed a marked reduction. The Br-IBAE process, on the other hand, significantly increased surface roughness. This increase in roughness was due to the highly anisotropic etch process in conjunction with thickness variations in the oxide layer and the large difference in etch rates between the oxides and the GaSb crystal itself.

4. Oxide composition results on the processed GaSb substrates

XPS spectra were obtained using a VG ESCALAB instrument equipped with a MgKα X-ray source and a concentric hemispherical analyzer detector. In-situ sputtering for depth profiling was done with a 5 keV argon ion gun with a typical ion beam current of ~100 μA, covering ~1 cm^2 sample area. The spectral region of interest for compositional analysis was 10–45 eV containing binding energies for both Ga 3d and Sb 4d. Due to the spin orbital splitting, the Sb 4d spectra shows two collocated binding energy peaks ($\frac{5}{2}$ and $\frac{3}{2}$) separated by 1.2 eV. For compositional analysis, the ratio of the two peak amplitudes was constrained to be 5:3 and their full-width at half-maxima (FWHM) to be the same. Published binding energies for Ga, Sb and their oxides, provided in Table 2, were acquired from the NIST database [13]. The spectra were fit to a Shirley background and deconvoluted using CasaXPS™. The complete removal of the surface oxides was confirmed by observing the diminished amplitude of the O 1s peak at 531.1 eV.

Fig. 1(a) and (b) shows the XPS spectra for a CMP produced surface layer at the surface and close to the

Table 1
Surface roughness for the processed GaSb surfaces

Process	Metric (nm)	Pre-process	Post-process
O_2-GCIB	R_a	0.25	0.38
	R_{rms}	0.32	0.5
	ΔZ	5.8	8.1
CF4/O_2-GCIB	R_a	0.28	0.18
	R_{rms}	0.35	0.22
	ΔZ	6	4.5
HBr-GCIB	R_a	0.41	1.75
	R_{rms}	0.31	2.17
	ΔZ	3.52	15.26
Br-IBAE	R_a	0.26	0.52
	R_{rms}	0.34	0.66
	ΔZ	7.6	12.9

Pre-process measurements represent CMP surfaces.

substrate/oxide interface, respectively. The composition of the surface layer showed a mixed Ga- and Sb-oxide that was ~11.4 nm thick requiring ~180 s of sputtering to remove. Depth profiling showed a stratification of Sb-oxides with a larger concentration of Sb_2O_3 towards the surface and Sb_2O_5 beneath it. This was most likely due to the conversion of Sb_2O_3 into the more stable Sb_2O_5 as evidenced by the heat of formation and Gibbs free energy values. Only Ga-oxides were found at the substrate/oxide interface.

The O_2-GCIB produced surface layer, shown in Fig. 2(a) and (b), was similar in composition and stratification to the CMP produced oxide with the exception it was ~28.6 nm thick and required ~250 s of sputtering to remove. Also, it was found that the thickness of the surface oxide layer increased proportionally with the fluence of O_2 clusters in the GCIB process. Here, the formation of a mixed Ga- and Sb-oxide distributed throughout its thickness was most likely due to O_2 molecules that were competing to form volatile compounds with the liberated

Ga and Sb, while also attaching themselves to the dangling bonds on the substrate. Thermal XPS (TXPS) measurements showed that the Sb-oxides were liberated from the surface by ~500 °C, by observing the Sb 3d peaks, leaving only Ga-oxides on the substrate surface.

In contrast, the CF_4/O_2-GCIB produced a surface layer that was ~6.4 nm thick requiring ~30 s of sputtering to remove. XPS spectra for these surfaces, shown in Fig. 3(a) and (b), indicated the presence of fluorides on the surface, confirmed by observing the F 1s peak at 686 eV in the survey scan. The composition of the surface layer showed the presence of SbF_3 at ~36.2 eV [13] and a strong GaF_3 peak at ~22.1 eV. Though there is no published data for GaF_3 in this region, the survey scan shows the presence of a peak at 108 eV [13], consistent with the observation of GaF_3 on the surface. Depth profiling revealed that the fluorides resided mostly on the surface with a mixed oxide beneath it. In this case, both CF_4 and O_2 components of the gas clusters react with the dangling bonds on the substrate to simultaneously form oxides and fluorides. The fluorides, however, percolate towards the surface and limit further oxide growth. Once again, only Ga_2O_3 was observed at the interface. TXPS measurements revealed the presence of the F 1s peak up to substrate temperatures of ~300 °C with its amplitude completely diminished by ~400 °C. Observation of the Sb 3d peak showed that Sb-oxides were liberated at a substrate temperature of ~500 °C, leaving mostly Ga-oxides beyond this temperature.

The HBr-GCIB produced a ~12-nm-thick surface oxide layer requiring ~60 s of sputtering to remove. Fig. 4(a) and (b) shows the XPS spectra for these surfaces indicating the presence of a mixed Ga- and Sb-oxide on the surface along with a $GaBr_3$ peak at ~22.7 eV. Again, there is no published data for $GaBr_3$ in this region but it is consistent

Table 2
Binding energies of Ga, Sb, and its oxides in the 10–45 eV region obtained from the NIST database [13]

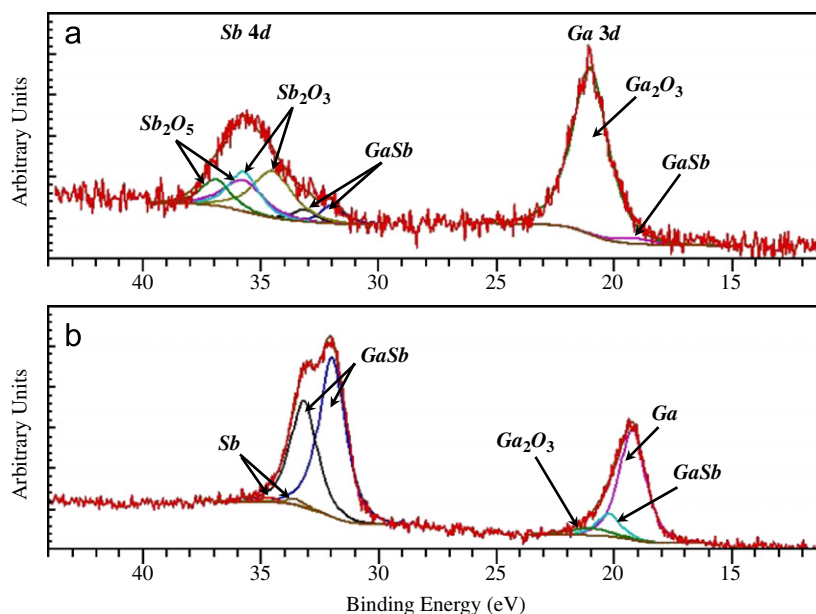| Element	Binding energy (eV)
Ga (3d $\frac{5}{2}$)	19.20
Ga (3d $\frac{5}{2}$) in GaSb	20.20
Ga (3d $\frac{5}{2}$) in Ga_2O_3	21.00
Sb (4d $\frac{5}{2}$) in GaSb	31.94
Sb (4d $\frac{5}{2}$)	33.44
Sb (4d $\frac{5}{2}$) in Sb_2O_3	34.50
Sb (4d $\frac{5}{2}$) in Sb_2O_5	35.70

Fig. 1. XPS data of CMP finished GaSb surfaces acquired: (a) at the surface and (b) near the substrate/oxide interface.
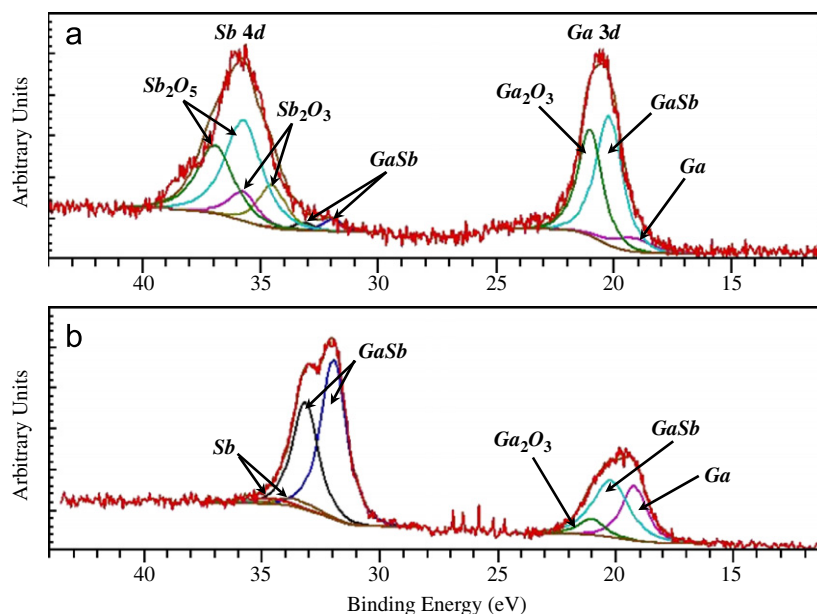
Fig. 2. XPS spectra of an O_2-GCIB finished GaSb surfaces acquired: (a) at the surface and (b) near the substrate/oxide interface.
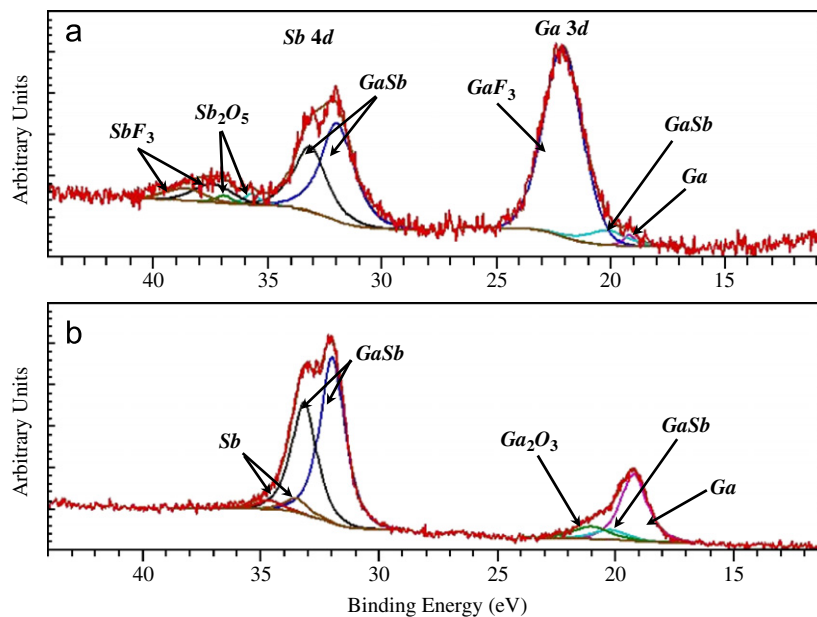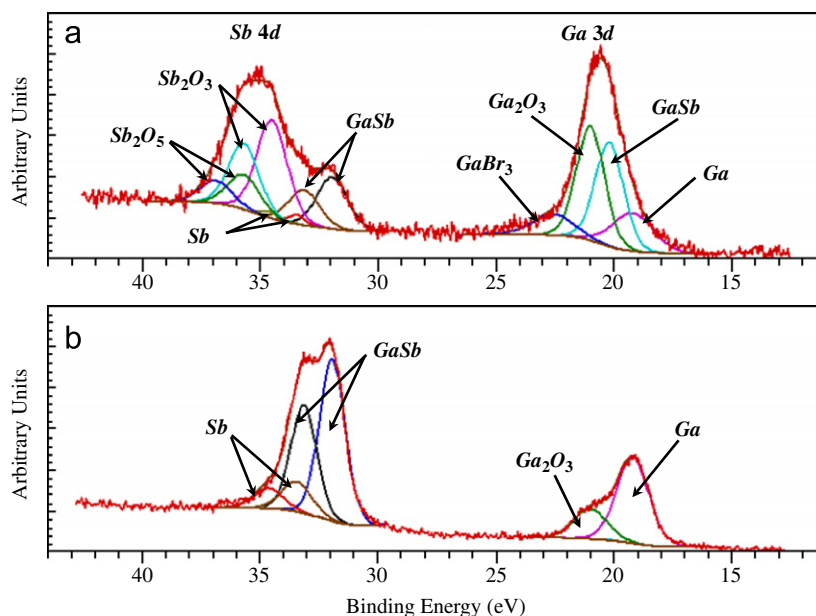

Fig. 3. XPS spectra of a CF_4/O_2-GCIB finished GaSb surface acquired: (a) at the surface and (b) near the substrate/oxide interface.

with the observation of a corresponding $GaBr_3$ peak at 106.8 eV in the survey scan [13]. Similar to the CF_4/O_2-GCIB finished GaSb surfaces, depth profiling showed that the bromides resided only at the surface with a mixed Ga- and Sb-oxide beneath it while only Ga_2O_3 was found at the interface. The composition of the Br-IBAE produced surface layers was similar in composition, except that it was the ~5.1 nm thick exhibiting a weaker $GaBr_3$ peak which required ~30 s of sputtering to remove. Observation of Br 3d and Sb 3d peaks during TXPS measurements showed that the bromides and Sb-oxides were liberated

from the surface by ~400 and ~500 °C, respectively, leaving mostly Ga-oxides beyond this temperature.

In general, thin Sb-rich oxides rather than Ga-rich oxides are preferred by the MBE community since they tend to desorb at lower temperatures, as evidenced by the thermal XPS measurements. However, Ga-depleted oxides begin to consume Ga atoms from the substrate over time to form a stable Ga-oxide at the substrate/oxide interface while simultaneously releasing the volatile Sb-oxide compounds [14]. This may well be the reason, why Ga_2O_3 was found at the substrate/oxide interface for all our samples.

Fig. 4. XPS spectra of a HBr-GCIB finished GaSb surfaces acquired: (a) at the surface and (b) near the substrate/oxide interface.

Thus, even though a surface modification process might produce thin Sb-rich oxides on an epi-ready GaSb substrate, it will eventually degrade to form Ga-oxides at the interface, thereby limiting its shelf-life.

5. Oxide desorption and epitaxial growth results

CMP, Br-IBAE, and GCIB finished GaSb substrates were indium bonded to a molybdenum substrate block at $\sim$200 °C in air. The substrates were introduced into the load/outgas chamber of the MBE system (Riber R&D2300) where they were heated to 300 °C and out-gassed at 5×10^{-8} Torr for $\sim$30 min. Of all the processed substrates, only the CF_4/O_2-GCIB surface exhibited heavy outgassing due to the presence of fluorine residues. The outgassed substrates were introduced into the growth chamber and brought up to 500 °C, with Sb flux introduced at 400 °C to provide a Sb-rich environment during oxide desorption and growth.

The surface oxide layers on the CMP and O_2-GCIB surfaces were successfully desorbed at 550 and 560 °C (substrate block thermocouple reading), respectively, while the oxides on the Br-IBAE, CF_4/O_2-GCIB, and HBr-GCIB surfaces desorbed at 530 °C. Oxide desorption was monitored by observing the development of characteristic antimony stabilized 2×8 streak patterns [15] on the reflection high-energy electron diffraction (RHEED) screen. While CMP, O_2- and CF_4/O_2-GCIB surfaces showed weak RHEED patterns, both Br-treated surfaces showed strong patterns consistent with efficient desorption. However, the substrate temperature in all cases was briefly raised to 560 °C to ensure complete desorption. Upon desorption, a substrate temperature of 500 °C was maintained during the growth run.

Flux measurements prior to epi growth indicated beam-equivalent pressures $\sim$2.9 $\times 10^{-7}$ Torr for Ga, $\sim$3.3 $\times 10^{-6}$ Torr for Sb, and $\sim$8 $\times 10^{-8}$ Torr for Al. Starting with a homo-epitaxial layer of GaSb, several periods of GaSb/AlGaSb layers were grown on the GCIB and Br-IBAE finished substrates with a final GaSb cap layer. The AlGaSb layers were used as marker layers to determine the evolution of the growing surface. Growth runs lasted 1 h with a growth rate of $\sim$1 μm/h. The epitaxial layers were characterized for crystal integrity using the (0 0 4) X-ray rocking curve measurements. The results showed that the substrate and alloy layer peaks were separated by $\sim$75 arcsec with the presence of several well-resolved satellite peaks indicative of good material crystallinity. Cross-sectional transmission electron microscopy (XTEM) of the epilayers were performed to evaluate the substrate/epi interface and the evolving epilayers.

Previously, results on the epitaxial growth on CMP finished GaSb surfaces had shown the presence of microvoids and stacking faults, while the O_2- and CF_4/O_2-GCIB finished surfaces showed a smooth substrate to epi transition but with the presence of a $\sim$600 Å wide dislocation layer and a discernable interface [10]. Fig. 5(a) shows a XTEM micrograph of epilayers grown on a typical O_2-GCIB-prepared surface. Presence of the dislocation layer was attributed to incomplete oxide desorption. Epitaxial growth on Br-IBAE and HBr-GCIB finished surfaces both showed extremely smooth substrate to epi transitions with no discernable dislocation layer or interface, as shown in Figs. 5(b) and (c), respectively. The absence of a dislocation layer is indicative of complete oxide layer desorbtion prior to epitaxial growth. Photoluminescence (PL) measurements at 77 K showed that the epilayers on GCIB finished surfaces exhibited an intensity
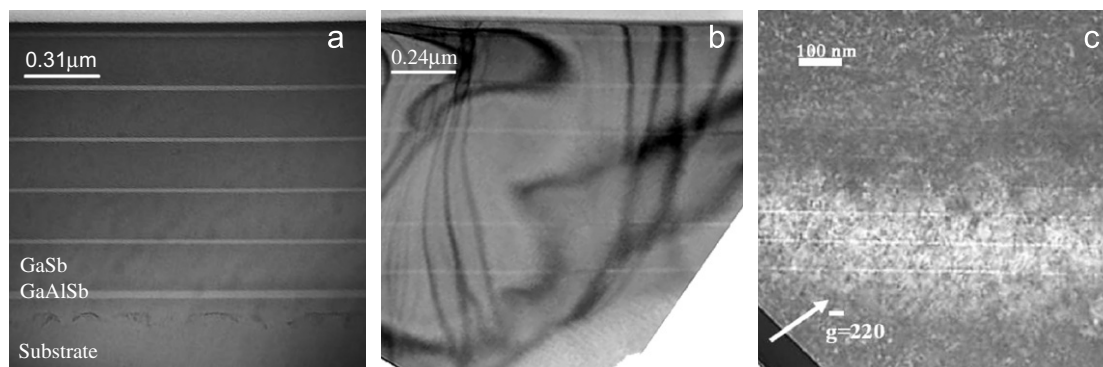
Fig. 5. XTEM images of GaSb/AlGaSb epi growth on: (a) O_2-GCIB; (b) Br-IBAE; and (c) HBr-GCIB finished GaSb substrates.

peak at ~1535 nm indicating single-crystal growth corresponding to a bandgap of 0.808 eV, comparable to the published values for dominant GaSb transitions of 0.796 eV [16]. Epi growth on the CMP surfaces showed no PL signatures.

The results of epitaxial growth, especially on the Br-processed surfaces, clearly highlighted the need for efficient oxide desorption at low temperatures in order to provide single-crystal templates for epitaxial growth. Furthermore, surface roughness of the substrate did not seem to impact interface quality and the evolving epilayers as self-planarization of GaSb in the 100 direction corrected any dislocation layer related defects.

6. Epitaxy surface topography results

Since the resultant topography of epi surfaces show some aspects of the initial template and others that are a function of the growth conditions, AFM images of epi surfaces were acquired to evaluate the quality of growth. AFM images with 10×10 and $1 \times 1 \mu m^2$ scan resolutions were acquired of epi surfaces grown on CMP-, Br-IBAE-, and GCIB-prepared substrates. Table 3 provides R_{rms} and ΔZ measurements for epi surface roughness.

Fig. 6(a–c) shows AFM images of CMP, Br-IBAE, and GCIB epi surfaces with a $10 \times 10 \mu m^2$ scan resolution. It can be seen that the CMP epi surface exhibited unevenly spaced steps and terraces with abrupt edges while the Br-IBAE epi surface showed the formation of concentric pyramid-like structures with sharp points at their apexes and other sharp points that were randomly distributed. Epi surfaces on the GCIB substrates exhibited a slowly undulating step-terrace formation.

Higher-magnification AFM images of the same surfaces, shown in Fig. 7(a–c), were acquired with a $1 \times 1 \mu m^2$ scan resolution. Here, it can be seen that the CMP epi surface exhibits meandering steps and terraces while Br-IBAE epi surface exhibited a high density of small, sharp point-like protrusions on pyramid-like formations. This formation was most likely due to the coalescing of atoms at screw dislocations at the interface resulting in sharp point-like features which, with subsequent growth, coalesce together

Table 3
Roughness of epi surfaces grown on the processed GaSb surfaces

Surface treatment	Metric	AFM scan resolution (μm^2)	
		10×10	1×1
CMP	R_{rms}	1.0	0.1
	ΔZ	6.9	0.9
Br-IBAE	R_{rms}	1.7	0.4
	ΔZ	12.0	6.9
GCIB	R_{rms}	0.7	0.1
	ΔZ	5.4	0.6

to form larger pyramid-like structures. The randomly located point-like structures that appear as speckles on the low-magnification images are due to the pyramids that did not fully coalesce with its neighbors and continued to advance with the epitaxial growth [17]. The GCIB epi surfaces exhibited the formation of uniform step-terraces with monatomic step heights and terrace widths on the order of ~0.1 μm. Wide terraces with monatomic step heights are commonly observed for extremely smooth surfaces [18]. Statistical analysis of GCIB epi surfaces showed self-similar random fractal behavior over eight orders of magnitude in the power spectral density with a fractal dimension of ~2.5 [19].

7. Summary of results

Based on our experimental results, we have shown that the GCIB surface treatment process is well suited for the production of epi-ready GaSb surfaces for the epitaxial growth. The choice of reactive gas in the GCIB process allows for reactively etching the substrate surface to remove CMP-induced damage while simultaneously producing an engineered surface oxide layer suited for MBE applications. The incorporation of Br as the reactive gas produced a thin-surface oxide layer that readily desorbed at 530 °C yielding a clean single-crystal template for epi growth.
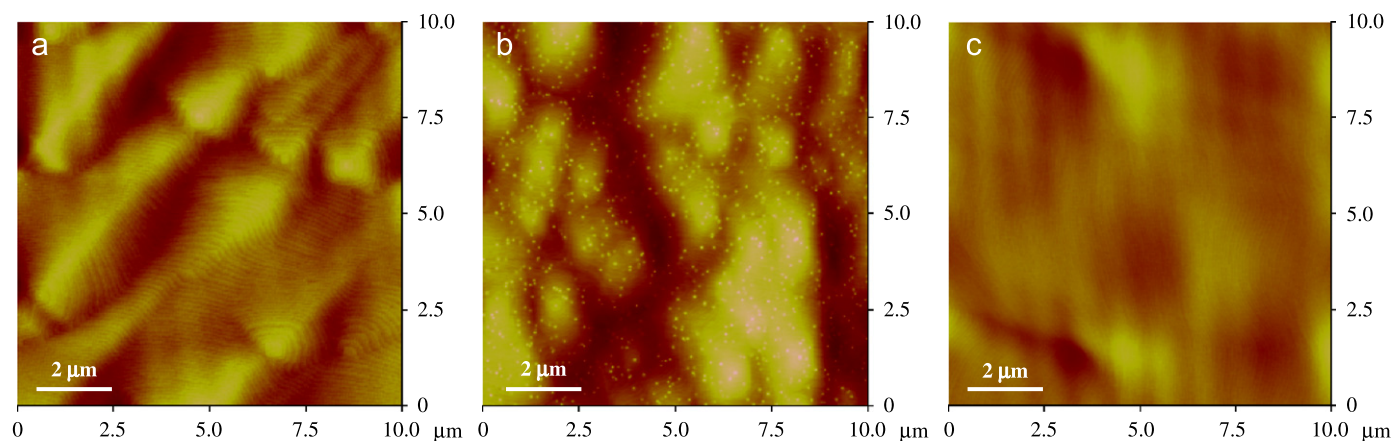
Fig. 6. AFM images with a scan resolution of $10 \times 10\,\mu m^2$ of the epi surfaces grown on: (a) CMP; (b) Br-IBAE and (c) GCIB processed GaSb substrates.
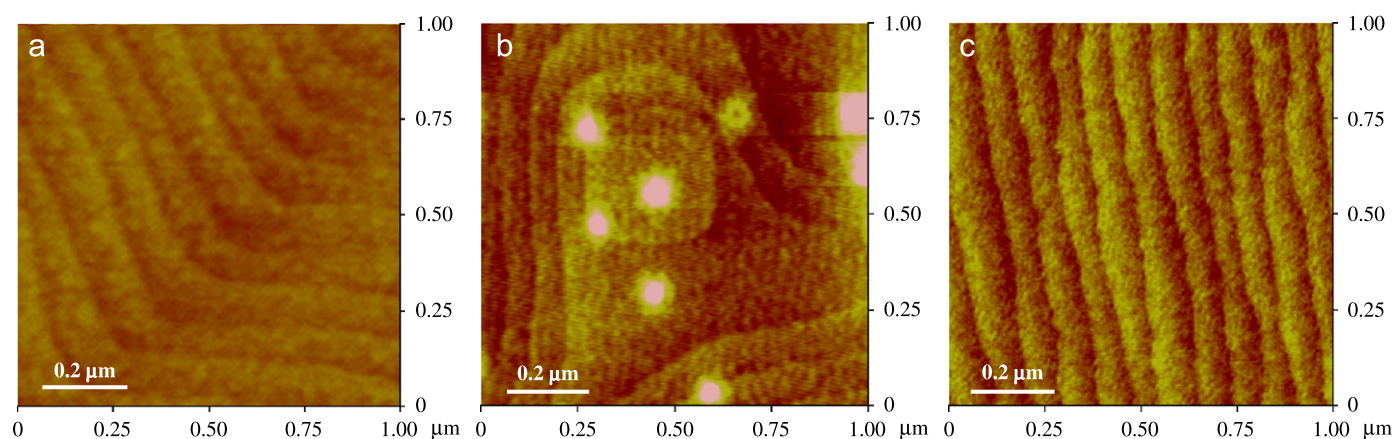

Fig. 7. AFM images with a scan resolution of $1 \times 1\,\mu m^2$ of epitaxial surfaces grown on: (a) CMP; (b) Br-IBAE and (c) GCIB finished GaSb substrates.

Microscopy of the substrate–epi interface showed that the HBr-GCIB surfaces exhibited smooth substrate-to-epi transitions with no discernable dislocation or interface layer, indicating complete oxide desorption prior to growth. Though the HBr-GCIB produced a rougher GaSb surface the tendency to self-planarize along the (1 0 0) direction resulted in a smooth epi surface exhibiting characteristic step-terrace formations with monatomic steps and wide terraces.

Even though the production of a well-behaved oxide layer is a priority, the importance of smooth surface templates cannot be understated. As evidenced by the epi surface topology results on the Br-IBAE surfaces, increased surface roughness results in the simultaneous growth along several crystal planes, therefore not benefiting from the self-planarization of GaSb. The HBr-GCIB process resulted in a minimal increase in the surface roughness, though not to the extent that it impacted the quality of epitaxial growth. Fine tuning the process parameters would certainly lead to surface finishes with reduced roughness and consequently improved epi surfaces. Finally, the HBr-GCIB can be easily adapted to a large-scale manufacturing process providing a path towards producing epi-ready GaSb surfaces.

Acknowledgments

References

[1] P.S. Dutta, H.L. Bhatt, V. Kumar, J. Appl. Phys. 81 (1997) 5821.
[2] M. Kodoma, Adv. Mater. Opt. Electron. 4 (1994) 319.
[3] Z.Y. Liu, B. Hawkins, T.F. Keuch, J. Vac. Sci. Technol. B 21 (2003) 71.
[4] M.A. Marciniak, R.L. Hengehold, Y.K. Yeo, G.W. Turner, J. Appl. Phys. 84 (1998) 480.
[5] C.A. Wang, D.A. Shiau, A. Lin, J. Crystal Growth 261 (2004) 385.
[6] E. Papis, A. Piotrowska, E. Kaminska, K. Golaszewska, W. Jung, J. Katcki, A. Kudla, M. Piskorski, T.T. Piotrowski, J. Adamczewska, Vacuum 57 (2000) 171.

[7] E. Papis, A. Kudla, T.T. Piotrowski, K. GOlaszewska, E. Kaminska, A. Piotrowska, Mater. Sci. Semicond. Process. 4 (2001) 293.

[8] N. Bertu, M. Nouaoura, J. Bonnet, L. Lassabatere, E. Bedel, M. Mamy, J. Vac. Sci. Technol. A 15 (4) (1997) 2043.

[9] G. Nagy, R.U. Ahmad, M. Levy, R.M. Osgood, M.J. Manfra, G.W. Turner, Appl. Phys. Lett. 72 (11) (1998) 1350.

[10] X. Li, W.D. Goodhue, C. Santeufemio, R. MacCrimmon, L.P. Allen, K. Krishnaswami, D. Bliss, C. Sung, Appl. Surf. Sci. 218 (2003) 251.

[11] K. Krishnaswami, S.R. Vangala, B. Zhu, W.D. Goodhue, L.P. Allen, C. Santeufemio, X. Liu, M.C. Ospina, J. Whitten, C. Sung, H. Dauplaise, D. Bliss, G. Dallas, D. Bakken, K.S. Jones, J. Vac. Sci. Technol. B 22 (3) (2004) 1455.

[12] S.R. Vangala, B. Krejca, K. Krishnaswami, H. Dauplaise, X. Qian, B. Zhu, M. Ospina, C. Sung, K. Vaccaro, D. Bliss, W.D. Goodhue, Mater. Res. Soc. Symp. Proc. 792 (2004) R9.2.1.

[13] NIST database for binding energies ⟨http://srdata.nist.gov/xps/⟩.

[14] Z. Wasilewski, J.-M. Baribeau, M. Beaulieu, X. Wu, G.I. Sproule, J. Vac. Sci. Technol. B 22 (3) (2004) 1534.

[15] A.S. Bracker, M.J. Yang, B.R. Bennett, J.C. Culbertson, W.J. Moore, J. Crystal Growth 220 (2000) 384.

[16] P.S. Dutta, B. Mendez, J. Piqueras, H.L. Bhatt, J. Appl. Phys. 80 (2) (1996) 1112.

[17] B.Z. Nosho, B.R. Bennett, E.H. Aifer, M. Goldberg, J. Crystal Growth 236 (2002) 155.

[18] K.F. Longenbach, W.I. Wang, Appl. Phys. Lett. 59 (19) (1991) 2427.

[19] K. Krishnaswami, D.B. Fenner, S.R. Vangala, C. Santeufemio, M. Grzesik, W.D. Goodhue, Mater. Res. Symp. 829 (2005) 273.